Organometallic Chemical Deposition of Crystalline Iridium Oxide Nanoparticles on Antimony-Doped Tin Oxide Support with High-Performance for the Oxygen Evolution Reaction

Ziba S. H. S. Rajan,[a] Tobias Binninger,[b] Patricia J. Kooyman,[c] Darija Susac[a] and Rhiyaad Mohamed*[a]

[a]*HySA/Catalysis Centre of Competence, Catalysis Institute, Department of Chemical Engineering, University of Cape Town, 7701, South Africa*

[b]*IBM Research – Zurich, Säumerstrasse 4, CH-8803 Rüschlikon, Switzerland*

[c]*Centre for Catalysis Research, Catalysis Institute, Department of Chemical Engineering, University of Cape Town, 7701, South Africa*

**Corresponding author. E-mail: rhiyaad.mohamed@uct.ac.za*

Electronic Supplementary Information

S1 X-ray Diffraction (XRD)

The XRD pattern below (**Figure S1**) that OMCD IrO_2/ATO does not show any distinguishable features from metallic iridium or iridium oxide components. Furthermore, the ATO diffraction pattern revealed no detectable metallic or oxidic antimony-based phases, thereby confirming the incorporation of the Sb-dopant atoms into the SnO_2 lattice. The feature which is present in between 30-40° in the XRD pattern for OMCD IrO_2/ATO is attributed to the background of the holder which was used for the acquisition of this particular diffraction pattern.

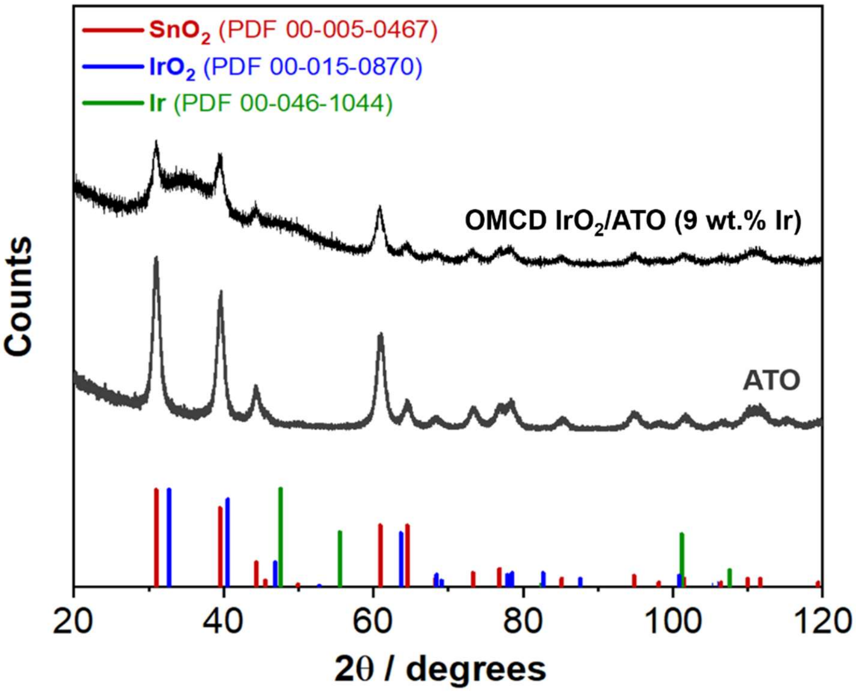

Figure S1. X-ray diffractograms of IrO_2/ATO and the blank ATO support. Reference patterns for SnO_2 (PDF-00-005-0467), IrO_2 (PDF-00-015-0870) and Ir (PDF-00-046-1044) metal are shown.

S2 Energy Dispersive X-ray Spectroscopy (SEM-EDX) Calibration Graph

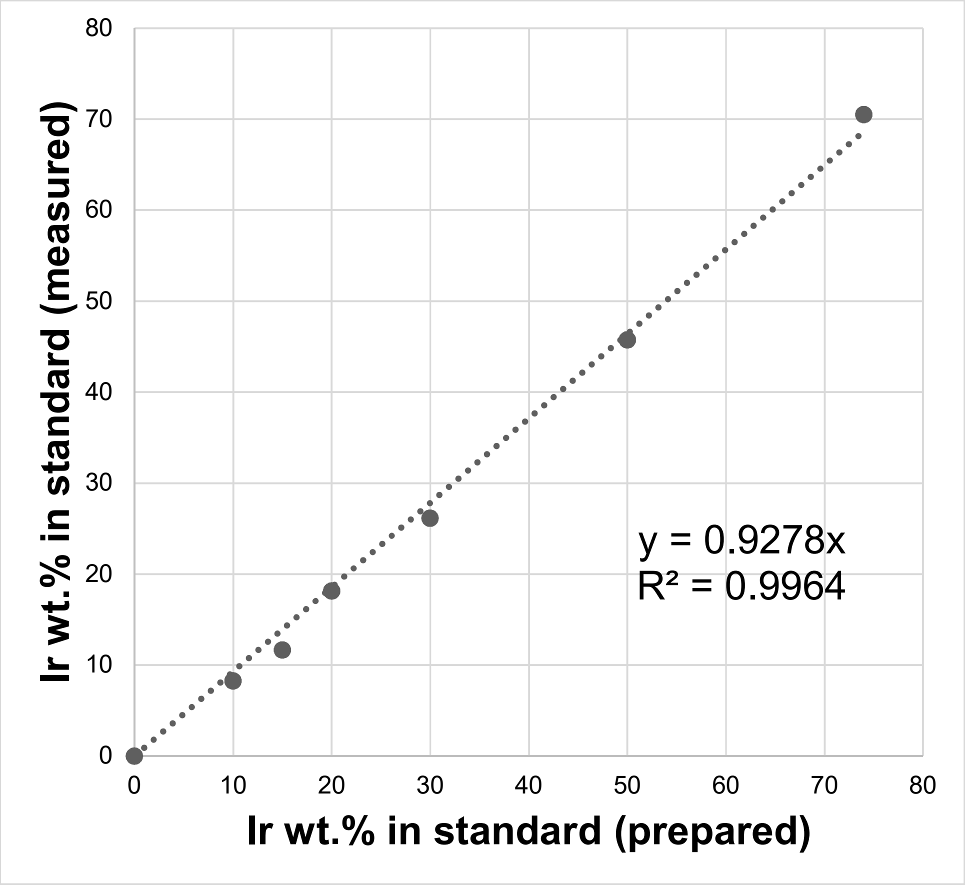

Figure S2. EDX calibration graph showing measured Ir mass loading by EDX versus known Ir mass loading in the prepared standards.

S3 Electrochemical Characterisation

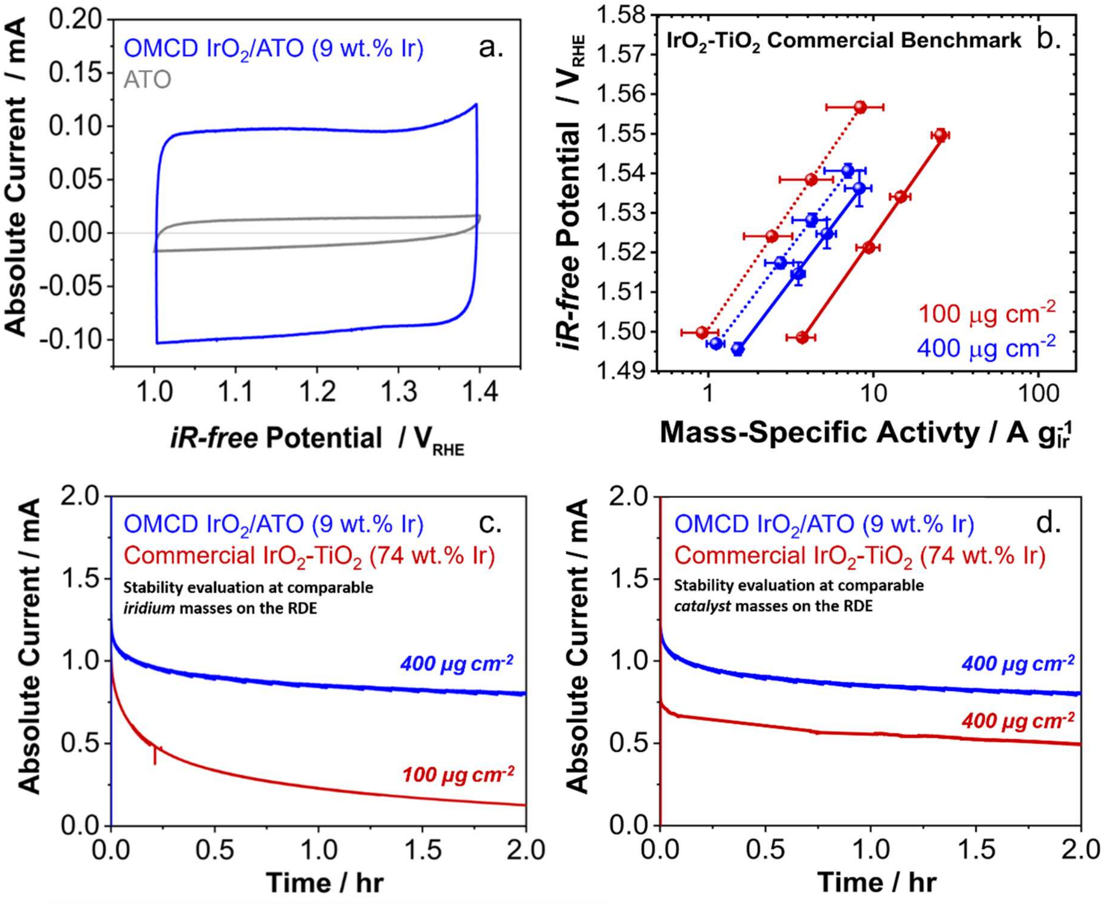

Figure S3. (a) Cyclic voltammetry from 1.000-1.400 V vs. RHE for OMCD IrO_2/ATO and blank ATO support. (b) Mass-specific Tafel plots of commercial IrO_2-TiO_2 benchmark, evaluated at two electrode loadings (100 and 400 µg cm^{-2}) before (solid lines) and after (dotted lines) stability experiments. (c-d) Comparisons of stability profiles of commercial IrO_2-TiO_2 for 2 hours at 1.600 V vs. RHE, when different electrode catalyst loadings of 100 µg cm^{-2} (c) and 400 µg cm^{-2} (d) for commercial IrO_2-TiO_2 were applied.

The results in Figure S3 (b) show that at the higher electrode catalyst loading of 400 µg cm^{-2}, the commercial IrO_2-TiO_2 catalyst exhibits lower mass-specific oxygen evolution activity in the *iR-free* potential range of 1.490-1.550 V vs. RHE compared to when measured with a lower electrode loading (100 µg cm^{-2}). After the stability test at 1.600 V vs. RHE, the opposite effect was observed: the lower catalyst loaded IrO_2-TiO_2 electrodes (Figure S3 (c)) degraded faster than the electrode prepared with higher catalyst loadings Figure S3 (d). A possible explanation for these results could be that in the case of the thicker electrode, evolved oxygen bubbles are not removed as rapidly and efficiently from the pores of the catalyst, as they are in the thinner electrode case, resulting in an overall lower rate of OER.

S4 Lattice Spacing Analysis

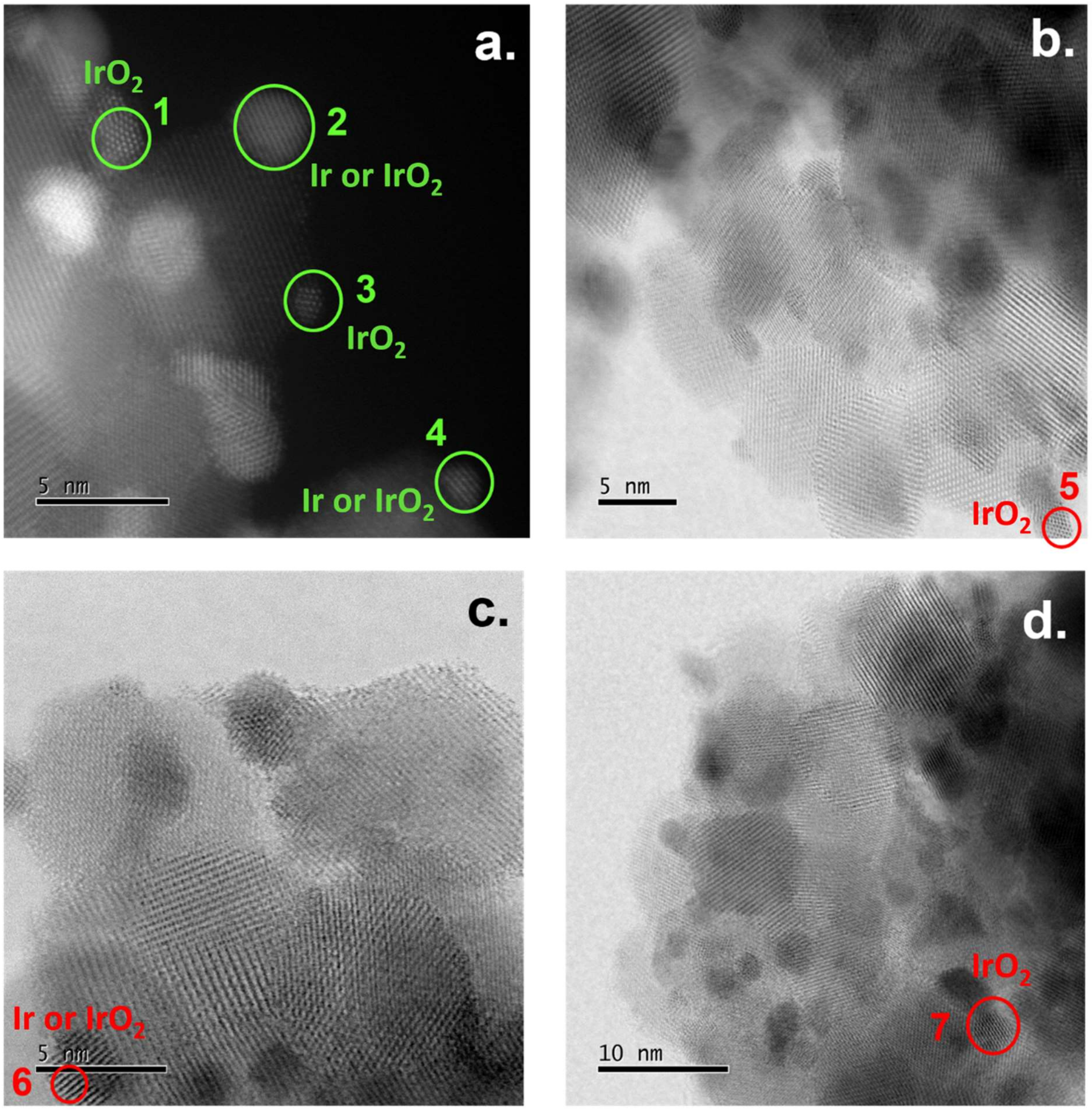

Figure S4. HR-STEM images used for determination of lattice spacings in OMCD IrO$_2$ particles. Image (a) is a HAADF image whereas images (b-d) are bright field images.

S5 Post-characterisation HR-STEM Images of OMCD IrO_2/ATO

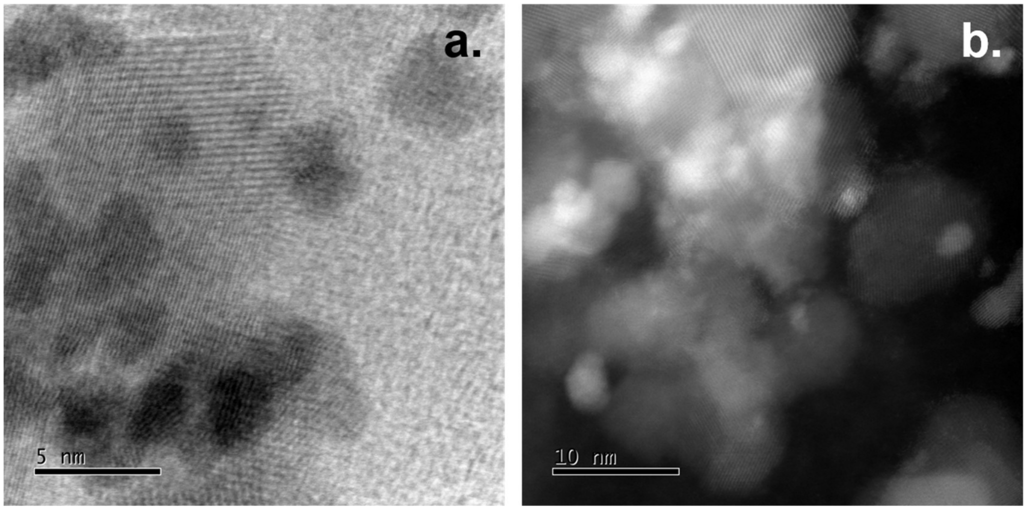

Figure S5. HR-STEM bright field (**a**) and HAADF (**b**) images of OMCD IrO_2/ATO after electrochemical characterisation.